Ocean Engineering 289 (2023) 116228

Contents lists available at ScienceDirect

Ocean Engineering

journal homepage: www.elsevier.com/locate/oceaneng

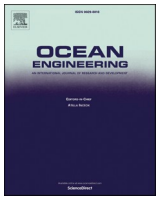

Topology optimisation of offshore wind turbine jacket foundation for fatigue life and mass reduction

Ali Marjan, Luofeng Huang *

School of Water, Energy and Environment, Cranfield University, Cranfield, MK43 0AL, UK

ARTICLE INFO

Handling Editor: Prof. A.I. Incecik

Keywords:
Topology optimisation
Offshore wind turbine
Jacket foundation
Aero-hydro-servo-elastic loads
Fatigue
Mass reduction

ABSTRACT

Offshore wind turbines are frequently regarded as a pricey source of electricity, and efforts are being made to lower both capital and operational costs by developing lighter and more robust structures. This paper presents a topology optimisation method to obtain a novel jacket foundation design by finding the optimum load path on the structure. The OC4 jacket model was computationally simulated considering the Aero-Hydro-Servo-Elastic loads, and the topology optimisation method was used to obtain a series of new designs. The structural optimisation is performed based on the dynamic response of the jacket, whilst restrained by relevant international design standards. In particular, time-domain fatigue simulations were performed to assess the structural integrity of the topology-optimised jacket for the first time. As a result, a range of optimised models with various thickness and diameter options are presented, which are shown to be rational and verify the optimisation procedure. The structural performance of the optimised geometry demonstrates the original jacket foundation is conservative, and the selection of optimised geometry achieved a mass reduction of 35.2% and simultaneously realised a 37.2% better fatigue life. The overall optimisation procedure and results provide useful practicalities for the design of offshore wind turbine foundations and potentially facilitate the structural integrity and cost reduction of the relevant industry.

1. Introduction

Global offshore wind projects are expected to grow more than tenfold by 2035, reaching a capacity of 519 GW. (World Forum Offshore Wind, 2023). The global offshore wind industry experienced its most successful year in 2021, adding 21.1 GW of new capacity worldwide (GWEC, 2022). The wind energy capacity of Europe has reached 255 GW, and 30 GW comes from offshore wind (WindEurope, 2023). Despite its huge potential, offshore wind energy is often criticized for its increased costs. The UK is facing criticism about the cost reduction track record due to supply chain pressures, cost increases due to inflation, higher interest rates, and the growing cost of project finance (The Crown Estate, 2022). However, the levelized cost of offshore wind has decreased from the historic high of 200$/MWh to a range of 61–116 $/MWh in 2021 (US Department of Energy, 2022). According to cost models, it may further decrease to $53/MWh by 2035 for the fixed-bottom offshore wind turbines (US Department of Energy, 2023). The support structure is the most critical part of the economics of offshore wind. The cost of support infrastructure can account for up to 21% of the total cost of the wind farm (Erik Morthorst, 2009; Musial and Ram, 2010). Initially, monopile foundations were used as the size of wind turbines was small. The cost of offshore wind technology is being reduced with the combination of innovative technology and the use of bigger wind turbines. Larger wind turbines required new projects to be installed in greater water depths. According to a cost comparison study by Damiani et al. (2016), monopile foundations are more cost-effective for water depths below 40 m. A jacket and floating foundations are often used for water depths greater than 40 m. The jacket structure is not only the most effective bottom-fixed structure but can also reduce the impact of wind and waves on the structure.

The offshore oil and gas sector has grown considerably; lessons are gained and applied to the offshore wind sector. However, the offshore wind industry lacks the historical knowledge and data sources to do that. Their designs were mainly based on the design codes and industry standards of the American Petroleum Institute (API) and Det Norske Veritas (DNV). Offshore wind turbine (OWT) jacket foundations are mostly four-legged, and their design was inspired by oil and gas jackets. Their design mainly follows International Electrotechnical Commission

* Corresponding author.
E-mail address: Luofeng.huang@cranfield.ac.uk (L. Huang).

https://doi.org/10.1016/j.oceaneng.2023.116228
Received 2 July 2023; Received in revised form 24 September 2023; Accepted 31 October 2023
Available online 6 November 2023

(IEC) regulations; IEC 61400-1, IEC 61400-3 (IEC, 2005; IEC, 2009); DNV standards like the Design of Offshore Wind Turbine Structures (DNV, 2014; API, 2014), and API Geotechnical and Foundation Design Considerations (API, 2014). However, the problem with these design codes is that they generate conservative and bulky designs, resulting in higher offshore wind costs.

Currently, efforts are being made to improve the designs of the jacket structure to enhance the structural integrity using different algorithms like gradient-based methods, level-set-based methods, and genetic algorithms. Kaveh et al. (Kaveh and Sabeti, 2017) used general Colliding Bodies Optimisation (CBO) and enhanced CBO (ECBO) methods to improve the design of OC4 jacket foundations. The jacket was modelled in 2D space with MATLAB, and a weight reduction was achieved by finding the optimal diameter and thickness. A similar study was performed by Häfele et al. (Häfele and Rolfes, 2016) using a particle swarm optimisation algorithm and found that the algorithm's efficiency was affected by the number of evaluated functions and load cases. However, the model only generated the designs at the conceptual level, and the structural design validation was not performed. The use of genetic algorithms to improve the design of offshore structures is discussed by Pasamontes et al. (2014). The study jointly optimised the member thickness, diameters, and locations of the nodes and found that the optimisation can be performed using the discrete values of the design variables from a catalogue. However, the author discovered that while the method produced lighter designs, many designs were not viable due to Stress Concentration Factors (SCFs) that exceeded the validity limits of the SCF calculation procedures. Savsani et al. (2021) used teaching-learning-based optimisation (TLBO) and genetic algorithms to optimise the jacket foundation and found that the efficiency of the TLBO algorithm is better than the genetic algorithm. Asgari et al. (Motlagh et al., 2021) used a genetic algorithm to optimise the design of the jacket foundation and achieved a 15% reduction in mass. However, their optimised structure exhibited failures at four locations before reaching the intended service life of 20 years. The genetic algorithm was also used to optimise the oil and gas jacket foundation to achieve an 8% weight reduction by Kling et al. (2019). The author liked the automated process and ease of implementation but emphasized the efficient use of mutations and design variables to reduce non-practical designs. Moreover, the parametric structural optimisation of a three-legged and a four-legged jacket was compared by Chew et al. (Hon Chew et al., 2013), who observed that a three-legged jacket optimisation could save more weight, but the fatigue damages are greater than the reference OC4 jacket foundation.

Topology Optimisation (TO) is a computational method used to generate an optimal distribution of material to achieve lightweight structures without compromising on structural integrity. The work by Meng et al. (2020) involved a review of TO methods and their application in additive manufacturing techniques. The researchers highlighted the trade-off between the ease of manufacturing and the unity of components in multi-functional products. Various literature studies show the growing use of TO and additive manufacturing in Aerospace (Satya Hanush and Manjaiah, 2022; Zhu et al., 2015), and the automotive industry (Jankovics and Barari, 2019a). TO is assisting in developing revolutionary aviation wings, fuselages, and engine components, and new suspension systems and chassis designs are being developed in the automation industry. Moreover, the use of TO in optimizing geometrically complex and aesthetically pleasing high-rise buildings is studied in (Jankovics and Barari, 2019b; Xie, 2022). TO is increasingly used in biomedical engineering as new implants and prostheses are being developed and 3D printed (Tan and van Arkel, 2021).

The use of TO in the offshore industry is relatively new but rising. Research is being done to optimise the offshore structures using the TO method to overcome the incapacity of some algorithms to model the complex nature of integrated aerodynamic and hydrodynamic loads. The jack-up offshore structures used in the oil and gas industry are optimised in (Deng et al.,2020; Tian et al., 2019) by maximizing the structural stiffness of the structure under extreme environmental conditions. The transition piece of a jacket foundation was optimised using TO by Lee et al. (2016), and the authors found that the TO model reduced the stresses by 15%. Tian et al. (2022) optimised the OC4 jacket foundation and also used shape and size optimisation to determine the size and diameters of the braces. A similar study was performed to optimise the topology of a jacket foundation; however, it was recommended to perform strength and fatigue checks in the future (Zhang et al., 2022). The research by Lu et al. (2023) showed the use of TO to optimise the tripod structure to extend the design life.

Due to the complicated and computationally intensive nature of the calculations, the use of TO in the offshore jacket design is underexplored. The relevant literature is limited, and several oversimplified assumptions were made during the simulation process; the applied loads are often derived analytically, and the complex dynamic interaction of different parts of the offshore wind turbine is ignored. Additionally, the published research suggested calculating fatigue damages and performing strength checks in future work. To address the existing research gaps, the present study focuses on calculating and implementing complex aerodynamic and hydrodynamic loads based on environmental data. The study contributes to the knowledge by introducing a novel framework that combines a series of software and computing the time-domain fatigue life of the topology-optimised design. As a result, time-domain fatigue simulations were conducted for the first time to assess the structural integrity of the topology-optimised jacket.

2. Methodology

A novel computational approach is established with a series of steps to optimise the existing model through TO and enhance fatigue life and material utilisation amount. The framework of the process and the use of different software modules are summarised in Fig. 1.

Sesam software was used in this study to model and analyse the jacket structure. Sesam was developed by DNV and is widely used in the offshore wind industry for modelling and analysis of offshore structures. Sesam also has modules for conducting structural modelling, dynamic analysis like modal analysis, and fatigue analysis of offshore structures. In this study, Sesam was utilised to model the jacket structure in detail, perform modal and static deflection analysis to verify the model, generate a super-element model to export to Bladed for load calculations, and ultimately estimate the fatigue damages on the optimised structure.

DNV Bladed software calculated the integrated wind turbine loads on the jacket structure. Bladed is an industry-standard software specifically developed for aerodynamic and aero-hydro-servo-elastic simulations of wind turbines. For this study, Bladed was used to calculate the detailed wind loads acting on the wind turbine rotor and tower and converted these as time series loads, which act at the interface node located between the tower and Transition Piece (TP). The complex simulations in Bladed help capture the multi-physics behaviour and provide accurate modelling of the integrated wind turbine system.

ANSYS software was specifically used for its TO module to produce innovative designs for the jacket structure. ANSYS is a popular FE software with advanced TO features. The key advantage of using ANSYS for TO is that it allows the creation of a continuum design space unconstrained by member connections. This enables the software to find the optimal load flow path without being limited by the initial design. In this study, ANSYS was used to conduct the TO of the jacket structure by defining the loads, design constraints, objectives, etc., to generate an innovative and optimised jacket design.

The rationale behind this selection of software tools is the seamless integration and interfacing between them, which enables efficiently conducting the complex multi-physics analysis required in this study. Sesam and Bladed are developed by DNV, and there are various verification studies performed by the DNV regarding the combined use of these software for industrial offshore applications. Moreover, it helps

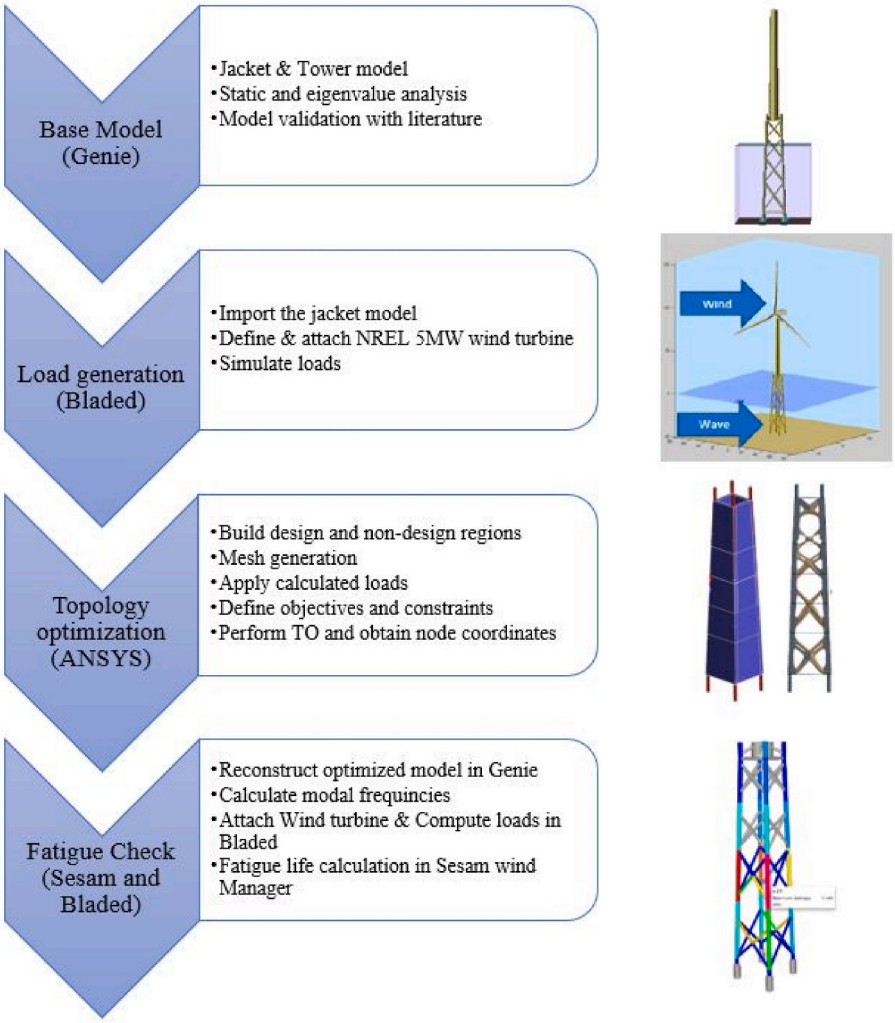

Fig. 1. Flowchart of the computational approach.

capture the accurate integrated loads in the time domain, which are often computed analytically in research studies. ANSYS provides the topology optimisation module to generate innovative designs.

2.1. Base model

2.1.1. Offshore wind turbine model

The NREL 5 MW wind turbine and an OC4 jacket foundation were selected for the analysis due to their widespread usage and the availability of publicly accessible data in (Jonkman et al., 2009) and (Vorphal and Kaufer, 2013). These models also offer many comparison studies for the validation of models and results. The rotor diameter of the wind turbine is 87.6 m, and the hub height is 90.55 m. The OC4 jacket is 70.15 m tall, and the piles are embedded 45 m in the soil. The jacket, soil, and tower models were developed in the Genie module of Sesam software, and the wind turbine model was generated in DNV Bladed. The wind-wave directionality effect has been ignored in this study to reduce the computational cost and the number of simulations. Moreover, the concrete TP has been replaced with steel beams having stiffness similar to the concrete because of Sesam's inability to model concrete elements. This ensured a similar effect on the model and was verified in the previous study by the author (Marjan and Hart, 2022). Moreover, a point mass was added at TP's location to obtain a total mass of 666 t. The main characteristics of the wind turbine and the jacket models are given in Table 1 and Table 2, respectively.

Table 1
NREL 5 MW wind turbine model (Jonkman et al., 2009).

Parameter	Value
Hub height	90.55 m
Rotor diameter	126 m
Orientation	Upwind
Cut-in speed	3 m/s
Cut-out speed	25 m/s
Rated wind speed	25 m/s
Tower height	87.6 m
Tower diameter top, bottom	3.87 m, 6 m
Tower thickness top, bottom	19 mm, 27 mm
Tower mass	347.46 t
Rotor nacelle assembly mass	350 t
TP mass	666 t

The analysis used the environmental and soil data from the K-13 deep water site given in Upwind Design Basis (Fischer and de Vries, 2010). The soil was modelled using a p-y method, and the author gave the details of the accuracy of this method for jacket foundations in a previous study (Marjan and Hart, 2022). The environmental and soil data of the K-13 site are given in Table 3 and Table 4, respectively, and a 3D model of the jacket foundation is given in Fig. 2.

2.1.2. Model verification

The base model was verified through Finite Element Analysis (FEA)

Table 2
OC4 jacket foundation properties (Vorphal and Kaufer, 2013).

Parameter	Value
Steel material density	7850 kg/m^3
Number of legs	4
Water depth	50 m
Young's modulus	2.1 x 10^{11} N/m^2
Buckling strength	355 MPa
Poisson's ratio	0.3
X-brace outer-diameter, thickness	0.8 m, 20 mm
Mud braces outer-diameter, thickness	0.8 m, 20 mm
Lowest level leg outer-diameter, thickness	1.2 m, 50 mm
Remaining legs outer-diameter, thickness	1.2 m, 35 mm
Piles outer-diameter, thickness	2.082 m, 60 mm
Jacket height	70.15 m
Grouted material density	2000 kg/m^3

Table 3
Environmental data of K-13 deep water site (Fischer and de Vries, 2010).

Parameter	Value
max wave height (50 years)	17.48 m
max wave period (50 years)	10.87 s
Significant wave height	9.4 m
Reference wind speed	42.73 m/s
Marine growth (-2 to -40 m)	100 mm
Marine growth density	1100 kg/m3
Normal current at sea level	0.6 m/s
Extreme current at sea level	1.2 m/s

Table 4
Soil data of K-13 deep water site (Fischer and de Vries, 2010).

Depth (m)	Young's modulus (MPa)	Friction angle (^{0})	Unit weight (N/m^3)
0–3	30	36	10000
3–5	30	33	10000
5–7	50	26	10000
7–10	50	37	10000
10–15	50	35	10000
15–50	80	37.5	10000

to obtain its eigenfrequencies and static deflection. The meshing is based on a beam element theory, and the Framework module later used for the fatigue damage calculation suggests two-node beam members. In beam element meshing, the focus is not on a certain mesh size but on the interconnected framework of beams with certain cross-sectional properties connected at the nodes. These kinds of elements are mainly used to capture the overall non-linear dynamics of the multi-body system, such as an offshore wind turbine. The accuracy of using beam elements in a multi-body dynamic system has been discussed by Wang et al. (2023). Moreover, beam elements are mostly used in structures that are mainly subjected to bending and axial loads but are not suitable to capture shear and torsional loads. Sesam default setting for meshing was used, which places the nodes at the end of the beam, and additional nodes are placed at the connection points and the edges of cans and stubs.

The results of four eigenfrequencies and deflections were compared with the corresponding data published by Damiani et al. (2013). The thrust load of 2 MN for the NREL 5 MW wind turbine found in (Damiani et al., 2013) along with the Rotor-Nacelle Assembly (RNA) point mass (350 t), was added at the top of the tower. Table 5 shows the model's prediction of the highest deflection values, compared with published data, showing a relative difference of 0.36%. Table 6 compares four natural frequencies and shows a maximum difference of 1.1%. The above comparisons indicate good accuracy of the present model. It was also confirmed that the natural frequencies do not approach most power-efficient regions for the wind turbine ($0.12 < 0.2$ or $0.35 < 0.61$ Hz) to avoid resonance (Marjan and Hart, 2022; Shi et al., 2015).

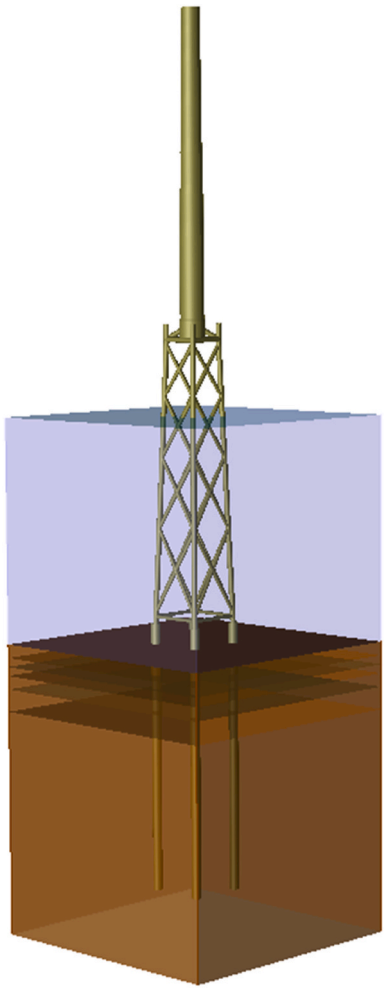

Fig. 2. 3D model of the jacket foundation.

Table 5
Verification of the maximum deflection.

Load case Thrust/RNA mass	Displacement at RNA		
	Current study	Published data (Damiani et al., 2013)	% Difference
2MN/350 t	1.204 m	1.209	−0.36 %

Table 6
Verification of the natural frequencies.

Models	Natural frequencies (Hz)			
	1st Fore-aft	1st Side-to-side	2nd Fore-aft	2nd Side-to-side
Present study	0.3169	0.3169	1.1799	1.1799
Published data (Damiani et al., 2013)	0.3189	0.3189	1.1936	1.1936
% Difference	−0.2%	−0.2%	−1.1%	−1.1%

2.2. Topology optimisation

2.2.1. Theoretical background

With the growing utility of Artificial Intelligence (AI) in technical advancements, designers are turning to AI to obtain cost effective whilst accurate predictions (Pena and Huang, 2021). A generative design process generates innovative designs that are unknown to designers

based on specific constraints and variables, including weight, size, material, and manufacturing method (Huang et al., 2022).

TO can improve existing or AI-generated designs by removing materials and generating an optimum load path under the specified constraints. The result is a lighter structure with similar structural integrity but a reduced mass and hence the cost. This approach is particularly useful when a structure faces multiple complex loads, like in the case of offshore wind turbines. A structure with the least deformation is considered a topology-optimised structure, achieved by increasing the stiffness (minimizing compliance). Mathematically, a TO problem can be written by Equation (1).

$$\min_{y} c(y) = V^T K V = \sum_{i=1}^{m} (y_e)^p V_i^T k_i v_i \; Subject\ to: \begin{cases} \dfrac{G_y}{G_0} = R \\ KV = F \\ 0 < z_{min} < z_j < 1 \end{cases} \quad (1)$$

Where k and v show the global displacement matrix and stiffness matrix respectively, y represents the design variables, K represents the stiffness matrix, z_{min} is the minimum relative density vector, F shows the overall stiffness matrix, p is the penalty factor, $G_{o,}$ and G_y represent the design area volume and overall material volume respectively, N represents the number of finite elements in the design area, and R is specified volume ratio (Deng et al., 2020).

The most common algorithm for TO is Solid Isotropic Material with Penalization (SIMP), where an optimal density is found for each element inside a design space. The conventional methods of optimisation result in the continuous variation of the density; however, the SIMP method forces the density near 0 or 1 by removing intermediate values with the help of a penalization method (Stroud, 2014). Level set-based optimisation is another approach for determining the structure's local minimal compliance. The focus of this method is to improve the shape and interface of the structure. This method is particularly useful where the structure may have holes, or the profile is split into several components. One drawback of this method is that volume conservation is not always achieved, resulting in a distorted shape (Perez, 2012). A mixable density algorithm combines the traits from the SIMP and level-set-based methods, but the SIMP method is often preferred due to the improved accuracy and reduced computational cost.

2.2.2. Loads calculation

TO is particularly useful when the loading conditions are complex, as in the case of OWT, where the structure is affected by the aerodynamic loads and thrust loads on the rotor, aerodynamic loads from the tower, aerodynamic and hydrodynamic loads faced by the foundation, complex transition of loads from the TP and non-linear soil-pile interaction. The wind loads encountered by the tower are calculated using Equation (2), and hydrodynamic loads can be calculated using Morison's equation (see Equation (3)). This equation helps calculate loads per unit length of the structure and combines drag and inertia forces.

$$F_{twr}(z) = {}^1\!/\!_2 \rho_a C_{D,T} V_i^2(z) D(z) \quad (2)$$

$$F_{wave} = F_d + F_m = {}^1\!/\!_2 \rho_w C_d D |U_x| U_x + \rho_w C_m \pi D^2/4 a_x \quad (3)$$

where $C_{D,T}$ shows the tower's drag coefficient and D(z) represents the tapered diameter of the tower at any height z, V_i represents the wind speed at hub-height, ρ_a and ρ_w indicate the density of air and water, respectively, C_d and C_m are drag and inertia coefficients, D is the member's diameter, u_x and a_x are velocity and acceleration induced by the current and wave.

Aero-Hydro-Servo-Elastic simulations are complex and capture the complex dynamic behaviours of different components of the OWTs. These simulations provide a dynamic response of the structure under the complex combination of structural, aerodynamic, and hydrodynamic loads. The simulations include the aerodynamic loads experienced by the rotor resulting from airflow, the hydrodynamic forces exerted on the offshore foundation, and the Servo-Elastic component, which involves the control system responsible for adjusting the wind turbine's operation within varying wind speeds and shutting it down beyond a specified cut-off wind speed. Furthermore, the simulation involves the structural response of the system, including vibrations, deflections, loads, and moments of the structure. In the previous studies in the field of TO, the loads are calculated analytically, and the integrated dynamic behaviour of the system has been ignored. The wind loads in this study are calculated using the DNV Bladed software, which is a wind turbine design tool offering aero-hydro-servo-elastic simulations for the OWTs. Moreover, it also helps in modelling a real wind turbine with accurate mass, location of the components, and blade profile. The complex Bladed simulation helps capture the model's multi-physics and holistically simulate the model (Manolas et al., 2020).

The jacket foundation model was generated in the Genie module of Sesam. The software allows the simulation to be performed using an integrated or super-element approach. In an integrated approach (used by (Glisic et al., 2018)), the tower model is also modelled along the jacket and exported to the DNV Bladed software to calculate the aerodynamic loads. However, only the jacket model is exported to the Bladed software along with the wave data to calculate the aerodynamic loads. DNV has also published verification studies showing the accuracy of both methods (DNV, 2019). This study uses a super-element method because this method is preferred in the industry as this can handle complex designs with ease (DNV, 2021a). A super-element mode includes information on the structure's mass, stiffness matrix, and gravity vector, along with the location of the interface node between the jacket and the tower. Moreover, the 3D and interface models should show similar spatial and spectral behaviour. This method and verification of the OC4 foundation have been performed in the previous study by the author (Marjan and Hart, 2022). Fig. 3 shows the visual differences between Bladed's super-element and integrated models. The exported super-element model is attached to the NREL 5 MW wind turbine model defined in Bladed. An external controller was also developed to obtain accurate results because the Bladed built-in controller cannot handle complex simulations.

The extreme loading conditions with the 50-year return period given in Table 3 are used to generate a design that can handle extreme conditions. The output of Bladed simulations is the time series of forces and moments in the x,y, and z directions. The maximum value of these loads in each direction is listed in Table 7.

The hydrodynamic loads and the wind loads on the jacket were calculated in Genie by applying the environmental conditions with a 50-year return period. The designers select the 50-year return period to ensure that the OWTs can withstand the extreme loading condition that may occur once in 50 years to achieve better structural integrity. Only the maximum load was calculated since the hydrodynamic load varies at a given wave period. The output is a line load that varies with the water depth and is given in Fig. 4. Moreover, the wind load on the jacket is 3800 N/m.

2.2.3. Topology optimisation process

Topology optimisation of the jacket foundation was performed using ANSYS software. It has been decided that the jacket will have four legs, and the brace design will be improved. Fig. 5 compares the original model with the TO design space in ANSYS. The structure was modelled as a continuum design space, and the legs' geometry was taken from the original model. Only the continuum design space will participate in the TO (Blue region), while the legs will only contribute to the overall structural stability (red region). The internal area of the jacket was also removed to ensure that the design was consistent with the original model. The tower, RNA, and TP masses are combined and act as a point mass on the jacket's interface node. Aerodynamic forces and moments are also applied at the top of the jacket. Moreover, sufficient mesh quality was ensured because it can greatly impact the accuracy of the

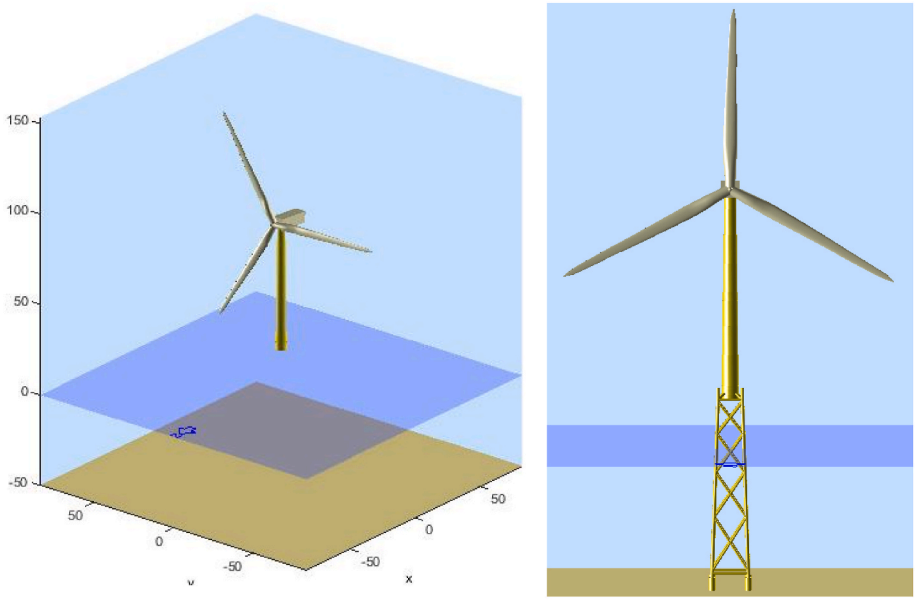

(a) Super-element model (b) Integrated model

Fig. 3. NREL 5 MW wind turbine model in Bladed.

Table 7
Aerodynamic loads (50 years return period).

F_x (kN)	F_y (kN)	F_z (kN)	M_x (kNm)	M_y (kNm)	M_z (kNm)
488	−132	−5480	9118	33739	−1668

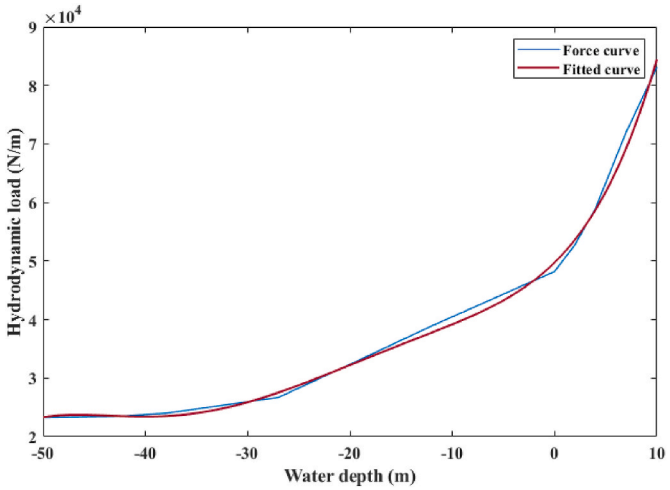

Fig. 4. Extreme hydrodynamic loading curve in a 50-year return period.

optimised structure. The jacket legs are thin, and a mid surface was extracted to achieve a better mesh.

A TO approach mainly aims to save cost by reducing mass without compromising structural integrity. The maximum displacement constraint is introduced at the interface node of the jacket to achieve maximum stiffness, as given in Equation (4).

$$d_{max} = d \tag{4}$$

Where d is the allowable displacement of the jacket's interface node, and d_{max} is the maximum displacement of the interface node. The stiffness increases because the structure is not allowed to displace as it normally would in the absence of constraint under a specific loading condition.

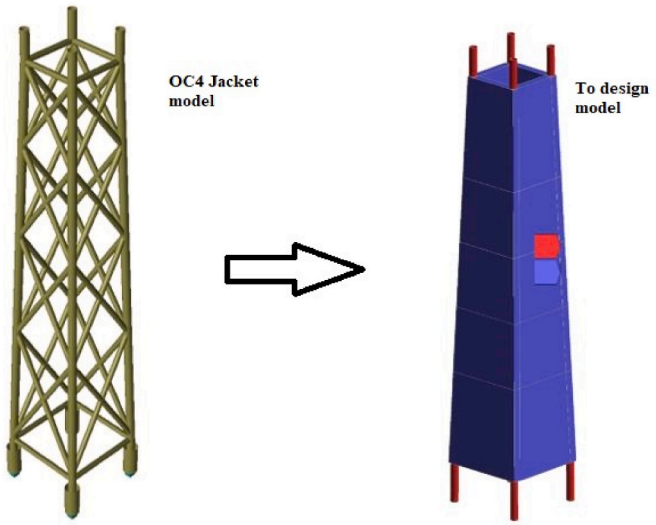

Fig. 5. Representation of OC4 jacket model and TO design space.

Typically the maximum displacement of the jacket is kept under 1/200 of the jacket height (Tian et al., 2022). The maximum allowable displacement in this study is constrained at 0.15 m. In addition, the stress is limited by a design constraint, and the upper limit is the buckling strength of the jacket (see Table 2).

The TO algorithm may develop designs with small non-manufacturable components, so a manufacturing constraint of minimum member size (1.4 m) was introduced, which also helps achieve a truss-like structure. The objective function is to minimize compliance (increase stiffness) with a displacement formulation type. A response constraint is also introduced to achieve 35% of the original mass of the optimisation region. Finally, a design constraint with cyclic repetition having four sectors was introduced to achieve a uniform design on all sides.

After 174 computationally intensive iterations, the solution converged, yielding a 5-tier x-brace jacket instead of a 4-tier OC4 jacket. Fig. 7 demonstrates that the retained region of the optimisation domain

increases after each iteration until the defined objective criteria are met. It is worth noting that the final shape of the TO is not the final product; it just gives the optimum load path for the jacket. The final shape needs to be reconstructed and compared with the original model. Furthermore, the final shape is not constrained by equal distance and angle between the braces, as is the case for the original model that follows DNV and API standards (DNV, 2021b; API, 2005). Table 8 compares the height co-ordinates of each brace to the original model.

2.2.4. Fatigue damage calculation

Properly defining joints is critical in fatigue calculation based on the hotspot stress approach. A joint is a sophisticated concept encompassing information about the structural joint and details of reinforcement data in cans and stubs. For a typical joint, an increase in the yield strength or wall thickness/diameter is increased for the chord as reinforcement. When the members have equal diameters, the thickness of one member is augmented to function as a toughness member, while the other members are considered minor members (Miranda, 2017). Moreover, when two or more members possess similar wall thicknesses, the member with the larger diameter is designated as the toughness member.

The joint concept is mostly introduced as a can and stub for a welded tubular joint, which can normally have a larger diameter and act as a toughness member, and a stub is a smaller diameter section which acts as a secondary member. API (API, 2014) and NORSOK (Norsk et al., 2014) standards have outlined some rules for the joint design, which are followed in the offshore wind, and oil and gas industries. The standards suggest that the minimum can length should be a minimum of one-fourth of a chord diameter, or 0.3 m. Similarly, stub length can be the same as stub diameter and should not exceed 0.6 m. This study has followed the rules suggested by the standards, and all the requirements for can/stub lengths, minimum gap, and cone dimensions were followed. Moreover, the toughness member was introduced on the x-joints as an increase in thickness, while a combination of an increase in thickness and diameter has been used for other joints. Fig. 8 visually represents the joint concept for a K joint and an X joint.

The locations of each x-brace were found from the topology-optimised model, and the model was reconstructed in Sesam's Genie module (See Fig. 6). The modified model's modal frequencies and static deflections were computed to compare with the original model and to see if the resonance zone was avoided. Sesam Wind Manager (SWM) generated the super-element model, which was then exported to Bladed. The aero-hydro-servo-elastic loads were calculated in Bladed by attaching an NREL 5 MW wind turbine, and these loads were imported into the SWM to calculate fatigue damages. The damages were calculated using the Framework module of the SWM using the S–N curve method. The estimation of member damages was based on the DNV2010_D S–N curve, while the computation of damages on the tubular joints utilized the DNV2010_T curve. These S–N curves are given in the DNV-RP-C203 standard (DNVGL, 2010), which provides recommendations for the fatigue design of offshore structures and helps choose the right S–N curve for different conditions and materials.

Table 8
Location of braces in OC4 and optimised model.

Variable	OC4 locations (m)	Optimised model locations (m)
Z1	15.6	15
Z2	4.3	9
Z3	4.4	5
Z4	−8.8	−2
Z5	−8.9	−4
Z6	−24.5	−12
Z7	−24.6	−18
Z8	−43.1	−29
Z9	–	−33
Z10	–	−44

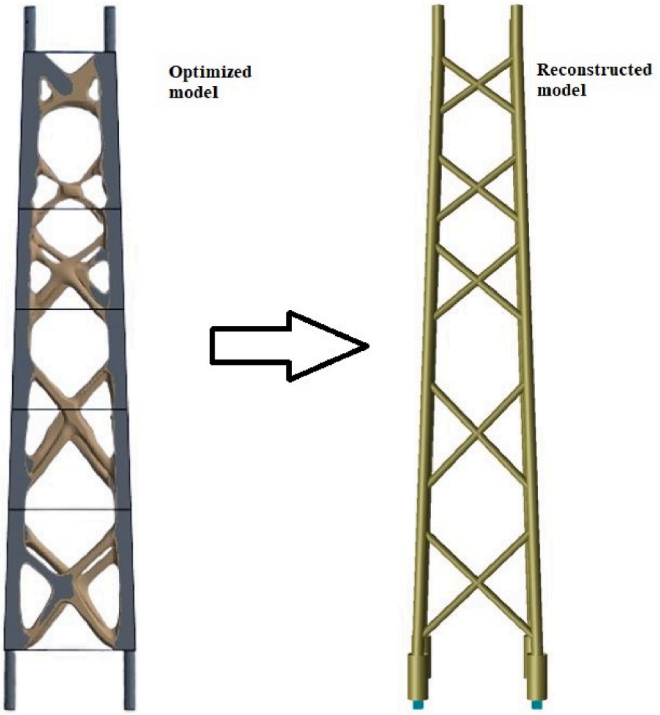

Fig. 6. Reconstructed model in Genie.

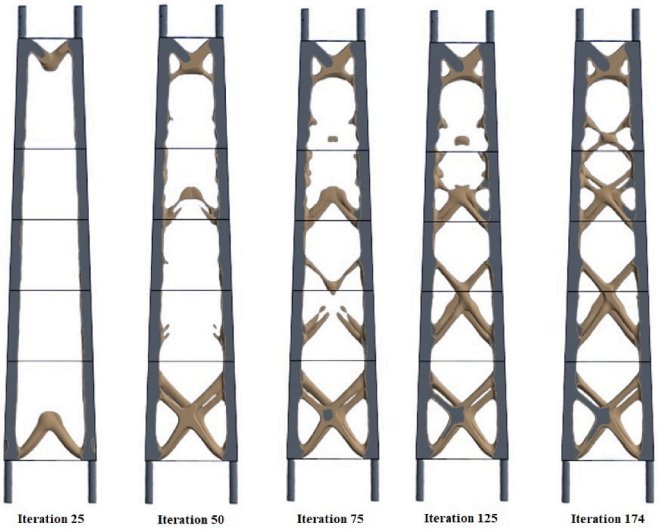

Fig. 7. Topology optimisation iterative process.

Moreover, a splash zone was also defined, and the software ensures that the S–N curve without cathodic protection is applied above the splash zone, while an S–N curve with cathodic protection is used underwater. The fatigue damages were accumulated for 20 years, and the member/joint is considered to fail when the damage value reaches one.

3. Results and discussion

3.1. Parametric models

The original OC4 jacket model was developed to compute and compare the eigenfrequencies and fatigue damages. Subsequently, the joints in the OC4 model were defined by adding cans and stubs. The original mass of the OC4 jacket, without considering the joint definition,

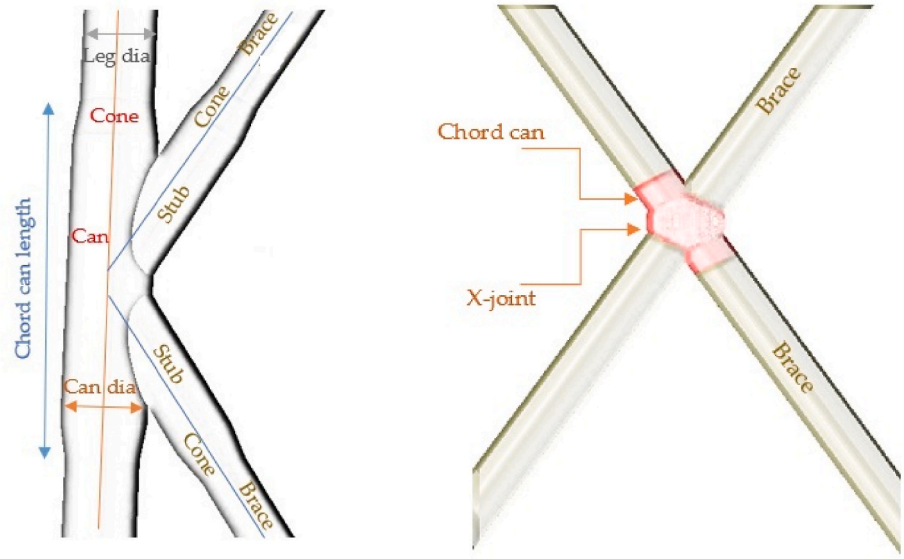

(a) K-joint (b) X-joint

Fig. 8. Visual representation of joints and locations of cans/stubs.

was 674 t. However, after increasing the thickness of the joint members (cans/stubs) by 5 mm, the mass increased to 718 t. This adjustment was made to assess fatigue life accurately and facilitate a comparison with topology-optimised models.

As the TO only provides an optimised flow path without providing details about the members' dimensions, different models were created with varying section properties of the members and joints. There are no specific instructions in the standards regarding the values of diameter or thickness. However, to ensure adequate strength, the offshore standards enforce limitations on the diameter-to-thickness (D/t) ratio. Norsok N-004 (Norsk et al., 2014) and ISO19902 (International Organization for Standardization, 2020) suggest that D/t should be less than 120. The standard guidelines were followed, and the D/t ratio was kept below 120.

The structural integrity of various models was evaluated by systematically reducing the dimensions of the jacket, resulting in a gradual decrease in mass until failure occurred. In this manner, the impact of varying section thickness and the combined influence of thickness and diameter variations on fatigue damages were examined.

Fig. 9 visually represents the position of various jacket sections, while the location of cans/stubs was shown earlier in Fig. 8. The dimensions of various sections used to examine the influence of thickness variation on fatigue damage are given in Table 9, and Table 10 presents the section properties used to examine the combined effect of thickness and diameter variation on fatigue life. The model name denoted by T indicates the models with thickness variation, and TD represents the models with thickness and diameter variation. Additionally, the joint parameters are listed as the dimensions of joint cans and stubs (see Fig. 8).

3.2. Dynamic behaviour analysis

The natural frequencies of vibration are a critical parameter governing the structural integrity of offshore wind turbines. Natural frequency refers to the frequencies at which a structure vibrates the most, thus it is essential to avoid the natural frequencies coincident with the frequencies of environmental loading. Their values are mainly affected by structural material and mass distribution, and higher natural frequencies imply greater stiffness. For offshore jacket wind turbines, the fore-aft and side-to-side frequencies are commonly used to refer to the natural frequencies in the longitudinal and transverse directions,

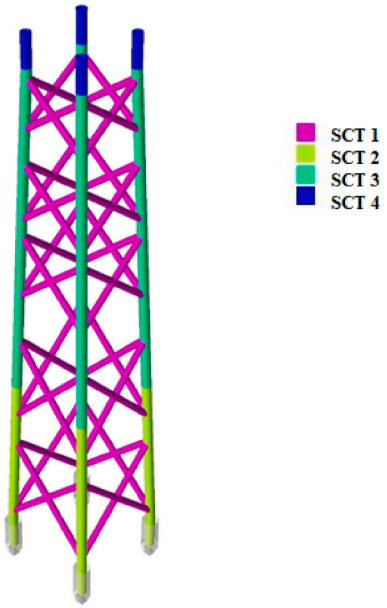

Fig. 9. Visual representation of the location of sections.

respectively (Marjan and Hart, 2022).

Properly designing the natural frequencies is essential to avoid resonance issues. A major requirement for a successful design is that the natural frequency of the optimised jacket should avoid the 1P and 3P frequency zones. The recommended practice is that the first two eigenvalue frequencies should most power-efficient regions for the wind turbine ($0.12 < 0.2$ or $0.35 < 0.61$ Hz) (Marjan and Hart, 2022; Shi et al., 2015). As presented in the above section, different models were generated by varying the thickness and diameter of essential components and their influence on natural frequencies are introduced below.

The eigenfrequencies predicted by the original geometry have been verified by available data of OC4 foundation in (Damiani et al., 2013) and a comparison is made with other optimised geometry in this study, as presented in Tables 11 and 12. Table 11 shows the effect of the thickness of members and joints (cans/stubs) on longitudinal and

Table 9
Section with thickness variation.

Model name	Brace D, T (mm)	Leg Sct-1 D, T (mm)	Leg Sct-2 D, T (mm)	Leg Sct-3 D, T (mm)	Leg_Can D, T (mm)	Leg_Stub D, T (mm)	Brace_Can D, T (mm)	Mass (Tonne)
Original	800,20	1200,50	1200,35	1200,40	1200,55	800,25	800,25	718
T-1	800,25	1200,50	1200,35	1200,40	1200,50	800,25	800,25	705
T-2	800,20	1200,40	1200,30	1200,30	1200,50	800,25	800,25	639
T-3	800,18	1200,35	1200,25	1200,25	1200,50	800,25	800,25	573
T-4	800,16	1200,30	1200,22	1200,22	1200,40	800,20	800,20	487
T-5	800,16	1200,32	1200,23	1200,23	1200,42	800,22	800,22	515
T-6	800,15	1200,28	1200,21	1200,21	1200,38	800,18	800,18	465
T-7	800,16	1200,24	1200,20	1200,20	1200,36	800,20	800,20	458

Table 10
Sections with thickness and diameter variation.

Model name	Brace D, T (mm)	Leg Sct-1 D, T (mm)	Leg Sct-2 D, T (mm)	Leg Sct-3 D, T (mm)	Leg_Can D, T (mm)	Leg_Stub D, T (mm)	Brace_Can D, T (mm)	Mass (Tonne)
TD-1	600,20	1000,40	1000,30	1000,30	1200,40	800,25	600,25	514
TD-2	600,18	900,35	900,25	900,25	1250,40	850,25	600,25	495
TD-3	550,16	800,32	800,25	800,25	1100,40	850,25	600,25	421
TD-4	570,17	850,32	800,25	800,25	1100,40	750,25	600,25	430
TD-5	570,17	850,32	820,25	820,30	1150,40	770,25	600,25	451
TD-6	600,18	900,35	900,30	900,30	1200,38	800,23	600,23	469
TD-7	600,17	850,32	850,30	850,30	1200,40	800,25	600,25	465

Table 11
Effect of thickness on natural frequencies.

Model name	1st fore-aft (Hz)	1st side-to-side (Hz)	2nd fore-aft (Hz)	2nd side-to-side (Hz)
Original	0.316	0.316	1.179	1.179
T-1	0.318	0.318	1.05	1.06
T-2	0.312	0.312	1.027	1.029
T-3	0.302	0.302	0.996	0.999
T-4	0.291	0.291	0.958	0.960
T-5	0.294	0.294	0.969	0.971
T-6	0.287	0.287	0.949	0.952
T-7	0.283	0.283	0.941	0.943

Table 12
Effect of thickness and diameter on natural frequencies.

Model name	1st fore-aft (Hz)	1st side-to-side (Hz)	2nd fore-aft (Hz)	2nd side-to-side (Hz)
Original	0.316	0.316	1.179	1.179
TD-1	0.297	0.297	0.961	0.963
TD-2	0.281	0.281	0.911	0.913
TD-3	0.261	0.261	0.822	0.825
TD-4	0.272	0.272	0.864	0.866
TD-5	0.279	0.279	0.882	0.885
TD-6	0.286	0.286	0.895	0.897
TD-7	0.282	0.282	0.881	0.883

transverse eigenfrequencies, while Table 12 presents the joint impacts of thickness and diameter. The results show that the optimised models have slightly lower natural frequencies due to lower mass, but the lower natural frequencies move further away from most power-efficient regions for the wind turbine ($0.12 < 0.2$ or $0.35 < 0.61$ Hz) (Marjan and Hart, 2022; Shi et al., 2015), thus having a benefit to structural integrity due to resonance avoidance. Yet, lower stiffness and can face greater movement under dynamic loads (Tian et al., 2022). Quantitatively, the 1st natural frequencies were lowered by around 10% due to the optimisation, and the 2nd were lowered by around 30%.

3.3. Fatigue damage assessment

A key consideration of designing and operating an offshore wind turbine jacket construction is fatigue analysis. The purpose of fatigue analysis of the optimised structure is to evaluate the impacts of cyclic loading over the wind turbine's operational lifetime. The fatigue damages for all joints and members are estimated using the previously stated S–N curves. The effect of thickness variation and the combined effect of diameter and thickness variation on fatigue damage is given in Table 13 and Table 14, respectively.

The fatigue damages ranged from 0.098 to 0.54 when only the thickness of the members and cans/stubs was varied. This reflects the level of damage induced by cyclic stress on the model, where fatigue damage value 1 implies structural failure over a 20-year fatigue life. Model T-1 exhibits the lowest damage, indicating an estimated fatigue life of over 100 years. This suggests that the design of T-1 is excessively conservative compared to the original model, which has a fatigue life of approximately 36 years. While T-2 and T-3 models achieve mass reductions of 11% and 20.19%, respectively, there is still room for further mass reduction in these models. By further reducing the thickness of the brace and legs, the T-4 model achieves a fatigue damage level comparable to the original model while also achieving a significant mass reduction of 32.17%. In the T-6 model, the thickness of the brace reaches a point where it cannot be further reduced without compromising its fatigue life. Similarly, in the T-7 model, reducing the thickness of the legs further would result in a decrease in the fatigue life below the desired 20-year lifespan. The Model T-5 is considered the most favourable since it offers a substantial mass reduction of 28.27% while maintaining relatively low fatigue damage even after 20 years of operation.

By decreasing members' diameter and thickness while simultaneously strengthening the joints, there is a greater opportunity to reduce the overall mass without compromising the structural integrity. This

Table 13
Effect of thickness variation on fatigue damages.

Model name	Fatigue damage	Failure location	Mass reduction (%)
Original	0.51	Brace-Joint	–
T-1	0.098	Leg-Joint	1.81
T-2	0.1	Leg-Joint	11
T-3	0.15	Leg-Joint	20.19
T-4	0.54	Brace-Joint	32.17
T-5	0.31	Brace-Joint	28.27
T-6	1.3	Brace-Joint	35.24
T-7	1.03	Leg-Joint	36.21

Table 14
Effect of diameter and thickness variation on the fatigue damages.

Model name	Fatigue damage	Failure location	Mass change (%)
Original	0.51	Brace-Joint	–
TD-1	0.35	Brace-Joint	28.4
TD-2	0.19	Brace-Joint	31.05
TD-3	1.44	Sct3	41.36
TD-4	1.23	Sct3	40.11
TD-5	0.55	Sct3	37.18
TD-6	0.38	Brace-Joint	34.67
TD-7	0.32	Brace-Joint	35.24

approach permits an optimal balance between the required strength and stability, and mass reduction. TD-1 has slightly greater fatigue damage despite having a mass similar to T-5, which shows the benefit of achieving mass reduction by reducing the redundant diameter. In contrast, TD-2 has a reduced mass and much less damage due to its strengthened joints, enhancing both strength and durability. In the models TD-3 and TD-4, leg members fail before the joints, showing that further mass cannot be reduced from the members, and the structure is failing sooner than 20 years. By increasing the diameter and thickness in the TD-5 model, the fatigue life has been extended; however, the structure fails at the member location first. Nevertheless, a further increase in the size of cans/stubs and the diameter of the members has resulted in the extended fatigue life of TD-5. It was observed that there is a scope of decreasing the members' diameter to achieve around 35% mass reduction if the cans/stubs dimensions are kept closer to the original dimensions of the members, as is the case in TD-6 and TD-7 models.

To further analyse the influence of geometrical factors on fatigue damage, Figs. 10 and 11 present the results linked to diameter and thickness respectively. In Fig. 10, it is evident that a higher component diameter induces less fatigue, except for the diameter of leg sections where a lower diameter could yield less fatigue. This suggests that diameter optimisation of the jacket structure could focus on the leg section part. Fig. 11 demonstrates that an optimal thickness exists for almost all the components, namely a too high or too low thickness could induce more fatigue. This suggests the necessity to find the optimal thickness of each component in future studies.

Fig. 12 shows the contour of the fatigue damages of the TD-7 jacket model. The brace exhibits the most severe damage, with other braces also experiencing greater damage compared to the legs, revealing that the failure occurs at the x-joint of the brace. The fatigue damage on the chord of the x-joint measures 0.322, while the chord of the leg joint has a fatigue damage of 0.276. Additionally, the fatigue damage consistently shows higher values on the chord side than on the brace side. The highest fatigue damage is 37.2% lower than the original design.

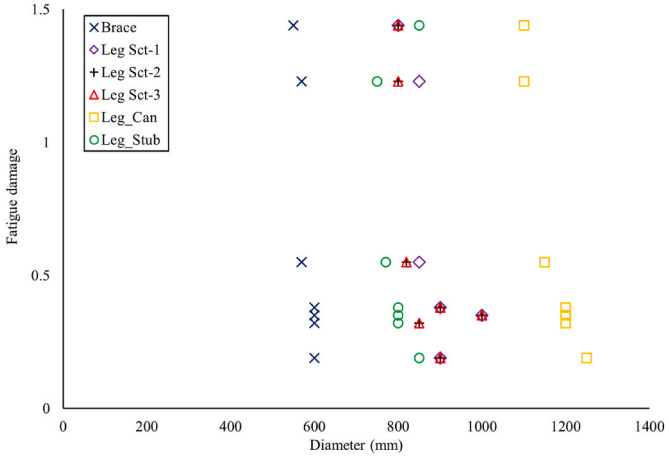

Fig. 10. The influence of component diameter on fatigue damage.

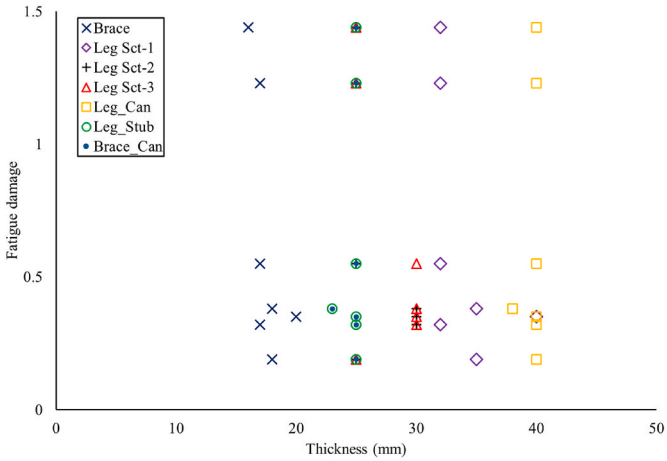

Fig. 11. The influence of component thickness on fatigue damage.

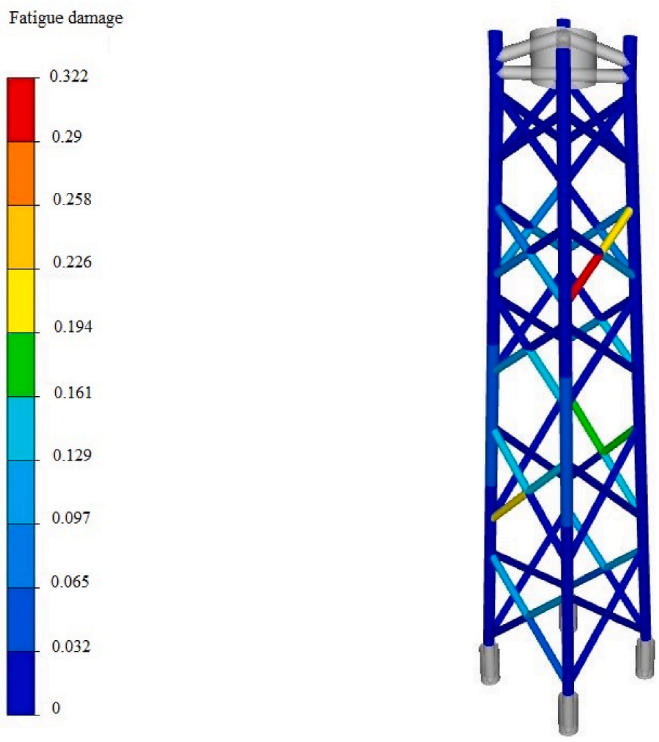

Fig. 12. Contour of fatigue damages of the TD-7 model.

The mass reduction could be obtained through the simplified process of thickness reduction only, but there is a scope for additional mass reduction if the diameter of the members is reduced with reinforced joints. Moreover, the accurate modelling of the joint plays a critical role in the extended design fatigue life of the jacket foundation. Based on the analysis performed in this study, TD-7 was the best model as it offered 37.2% lower fatigue damages but also offered around 35% mass reduction. Moreover, Model TD-7 achieves a considerably lower mass in comparison to the T-5 model, even though the fatigue damage levels are similar.

4. Conclusions

This paper explored the use of TO to optimise the existing OC4 jacket foundation, and the optimised model was used to estimate the fatigue damages using the hotspot stress approach. The jacket model was

developed in Sesam, and the environmental loads faced by the jacket were estimated using the Sesam and Bladed. A continuum model with legs from the original OC4 model was built in Ansys, and TO analysis was performed. The goal of the TO is to obtain an ideal flow path for the structure without much information about the dimensions. The TO process output under the defined constraints and loads was a five x-brace jacket structure. The model was rebuilt in the Sesam and exported again to Bladed for the load calculation. Furthermore, various models were developed to investigate the influence of the thickness and diameter of the members and cans/stubs on the fatigue life of the jacket. Eventually, Sesam Wind Manager estimated the fatigue damage on the members and joints based on the defined S–N curves.

The simulation results revealed that the TO process successfully produced a distinct truss-like structure. The optimised structure enables optimum load distribution and increases structural integrity overall. Furthermore, when evaluating the dynamic behaviour of the models, the first two eigenfrequencies were found to fall within a safe range of 0.22–0.35 Hz. In addition, it was noted that the higher-order natural frequencies of the models were also higher than the recommended threshold of 0.605 Hz. These frequencies falling inside the defined safe range indicate that the models have a good amount of stiffness and don't experience resonance.

The fatigue calculations of the reconstructed optimised structure suggested that the design is quite conservative. Additionally, reducing the members' thickness and diameter could result in a substantial mass reduction of up to 35% compared to the original structure while still maintaining a significant fatigue life. It was observed that the failure in the TD-3 and TD-4 models occurred at the members instead of the joints. This finding suggested that the failure of the structure would occur sooner than the desired operational lifespan of 20 years if additional reductions in member mass were attempted. The TD-5 model was built with the increased diameter and thickness; although the failure was still at the member, the fatigue life had almost doubled. Moreover, for similar fatigue damage, it is possible to achieve the additional mass reduction by decreasing the diameter and thickness of the members while simultaneously strengthening the joints, as opposed to when only the thickness of the members was varied.

In conclusion, a significant mass reduction could be achieved by using the TO approach, and the mass reduction is greater when the redundant diameter is also reduced along with the thickness of the members. To achieve this reduction, accurate modelling of joints plays a vital role, and it is essential to reinforce the joints with cans and stubs. This study successfully achieved a reduction in mass of approximately 35% while simultaneously reducing fatigue damages by 37.2% compared to the original OC4 jacket foundation.

The study focused on demontrating an innovative design approach by employing the TO and subsequently calculating fatigue life by integrating complex dynamic environmental loads. A series of high-fidelity simulation software is integrated for the first time. The application of TO in the design of offshore jacket foundations has not been extensively explored, making it an area with untapped potential. The published research is quite recent and suggests fatigue life calculation in the future. This research is the first to propose a framework that integrates TO with fatigue life analysis and provides computed results for the fatigue life of the innovative design. The comprehensive approach suggested by the research can help address the design challenges of cost-effective offshore jackets and tripod foundations.

However, the use of TO has a major disadvantage in terms of computational cost, especially considering dynamic fatigue calculations. Moreover, the final TO output can vary significantly if the constraints are changed or are modelled incorrectly, hence requiring the expertise of the designers. Moreover, this study considers the uni-directional wind and waves, whereas real conditions involve multi-directional loading, which may cause a discrepancy in prediction. Additional deviation may also arise with the inclusion of Computational Fluid Dynamics (CFD) models which are not considered in this study due to the computational cost in this research (García Auyanet et al., 2022; Liu et al., 2023; de Oliveira et al., 2023). In future work, Advanced AI-based models are recommended to further improve the optimisation algorithm and computational speed, thus including additional features to address the above-mentioned limitations (Huang et al., 2022).

CRediT authorship contribution statement

Ali Marjan: Conceptualization, Methodology, Software, Validation, Formal analysis, Investigation, Data curation, Writing – original draft, Visualization. **Luofeng Huang:** Methodology, Investigation, Resources, Writing – review & editing, Visualization, Supervision, Project administration, Funding acquisition.

Declaration of competing interest

The authors declare that they have no known competing financial interests or personal relationships that could have appeared to influence the work reported in this paper.

Data availability

All data underlying the results are available as part of the article and no additional source data are required.

References

API, 2005. Recommended Practice for Planning, Designing.

API, 2014. Geotechnical and Foundation Design Considerations.

Damiani, R.R., Robertson, A.N., Jonkman, J.M., 2013. Assessing the importance of nonlinearities in the development of. In: Proceedings of the International Conference on Offshore Mechanics and Arctic Engineering American Society of Mechanical Engineers, pp. 1–16. Nantes, France.

Damiani, R., Dykes, K., Scott, G., 2016. A comparison study of offshore wind support structures with monopiles and jackets for U.S. waters. J. Phys. Conf. Ser. 753 (9) https://doi.org/10.1088/1742-6596/753/9/092003.

de Oliveira, M., Puraca, R.C., Carmo, B.S., 2023. A study on the influence of the numerical scheme on the accuracy of blade-resolved simulations employed to evaluate the performance of the NREL 5 MW wind turbine rotor in full scale. Energy 283, 128394.

Deng, W., Tian, X., Han, X., Liu, G., Xie, Y., Li, Z., 2020. Topol. Optim. of Jack-up offshore platform Leg Struct. 235 (1), 165–175. https://doi.org/10.1177/1475090220928736, 10.1177/1475090220928736.

DNV, 2014. DNV-OS-J101 Design of Offshore Wind Turbine Structures.

DNV, 2019. Verification Report of Sesam ' S Bladed interface_IMPLEMENTING an INTERFACE between BLADED and SESAM Verification.

DNV, 2021a. "USING SESAM ™ AND BLADED IN ONE WORKFLOW.

DNV, 2021b. Support Structures for Wind Turbines.

DNVGL, 2010. Fatigue Design of Offshore Steel Structures RP-C203.

Erik Morthorst, P., 2009. THE ECONOMICS OF WIND POWER. Copenhagen.

Fischer, B.S.T., de Vries, W., 2010. Upwind Design Basis. North.

García Auyanet, A., Santoso, R.E., Mohan, H., Rathore, S.S., Chakraborty, D., Verdin, P. G., 2022. CFD-based J-shaped blade design improvement for vertical Axis wind turbines. Sustainability 14, 15343.

Glisic, A., Nguyen, N.-D., Schaumann, P., 2018. Fatigue analysis on innovative 10 MW offshore jacket structure using integrated design approach. In: THE INTERNATIONAL CONFERENCE ON WIND ENERGY HARVESTING, p. 269.

GWEC, 2022. Global Offshore Wind Report 2022.

Häfele, J., Rolfes, R., 2016. Approaching the ideal design of jacket substructures for offshore wind turbines with a Particle Swarm Optimization algorithm. In: Proceedings of the Twenty-Sixth (2016) International Ocean and Polar Engineering Conference. ISOPE [Online]. Available. www.isope.org.

Hon Chew, K., Muskulus, M., Zwick, D., Ng, E., Tai, K., 2013. Structural optimization and parametric study of offshore wind turbine jacket substructure. In: Proceedings of the Twenty-Third (2013) International Offshore and Polar Engineering Anchorage. ISOPE.

Huang, L., Pena, B., Liu, Y., Anderlini, E., 2022. Machine learning in sustainable ship design and operation: a review. Ocean Eng. 266, 112907.

IEC, 2005. International Standard IEC 61400-1 - Wind Turbines-Design Requirements.

IEC, 2009. Internation Standard IEC 61400-3 - Design Requirements for Offshore Wind Turbines.

International Organization for Standardization, 2020. ISO 19902:2020 - Petroleum and natural gas industries — fixed steel offshore structures [Online]. Available: https://www.iso.org/standard/65688.html. (Accessed 19 June 2023).

Jankovics, D., Barari, A., 2019a. Customization of automotive structural components using additive manufacturing and topology optimization. IFAC-PapersOnLine 52 (10), 212–217. https://doi.org/10.1016/J.IFACOL.2019.10.066.

Jankovics, D., Barari, A., 2019b. Customization of automotive structural components using additive manufacturing and topology optimization. IFAC-PapersOnLine 52 (10), 212–217. https://doi.org/10.1016/j.ifacol.2019.10.066.
Jonkman, J., Butterfield, S., Musial, W., Scott, G., 2009. Definition of a 5-MW reference wind turbine for offshore system development. Golden, CO (United States). http://www.osti.gov/bridge.
Kaveh, A., Sabeti, S., 2017. Optimal Design of Jacket Supporting Structures for Offshore Wind Turbines Using Enhanced Colliding Bodies Optimization Optimal Design of Jacket Supporting Structures for Offshore Wind Turbines Using Enhanced. Periodica Polytechnica Civil Engineering.
Kling, E.Y., Ferri, B., Bjørhovd, B., Strand, F., Hope, S.M., 2019. Automated jacket design. Proc. Int. Offshore Polar Eng. Conf. 1, 1062–1068.
Lee, Y.S., González, J.A., Lee, J.H., Il Kim, Y., Park, K.C., Han, S., 2016. Structural topology optimization of the transition piece for an offshore wind turbine with jacket foundation. Renew. Energy 85, 1214–1225. https://doi.org/10.1016/j.renene.2015.07.052.
Liu, Y., Ge, D., Bai, X., Li, L., 2023. A CFD study of vortex-induced motions of a semi-submersible floating offshore wind turbine. Energies 16, 698.
Lu, F., Long, K., Zhang, C., Zhang, J., Tao, T., 2023. A novel design of the offshore wind turbine tripod structure using topology optimization methodology. Ocean Eng. 280 (April 2022), 114607 https://doi.org/10.1016/j.oceaneng.2023.114607.
Manolas, D.I., Riziotis, V.A., Papadakis, G.P., Voutsinas, S.G., 2020. Hydro-servo-aero-elastic analysis of floating offshore wind turbines. Fluid 5 (4), 200. https://doi.org/10.3390/FLUIDS5040200, 2020, Vol. 5, Page 200.
Marjan, A., Hart, P., 2022. Impact of design parameters on the dynamic response and fatigue of offshore jacket foundations. J. Mar. Sci. Eng. 10 (9), 1320. https://doi.org/10.3390/JMSE10091320, 2022, Vol. 10, Page 1320.
Meng, L., et al., 2020. From topology optimization design to additive manufacturing: today's success and tomorrow's roadmap. Arch. Comput. Methods Eng. 27 (3), 805–830. https://doi.org/10.1007/s11831-019-09331-1.
Miranda, F.M.B., 2017. Finite Element Analysis of Tubular Offshore X-Joint under Static Loading.
Motlagh, A.A., Shabakhty, N., Kaveh, A., 2021. Design optimization of jacket offshore platform considering fatigue damage using Genetic Algorithm. Ocean Eng. 227 (March), 108869 https://doi.org/10.1016/j.oceaneng.2021.108869.
Musial, W., Ram, B., 2010. Large-Scale Offshore Wind Power in the United States: Assessment of Opportunities and Barriers. https://doi.org/10.2172/990101. Golden, CO (United States).
Norsk Sokkels Konkuranseposisjon, 2014. Design of Steel Structures. https://doi.org/10.1002/9783433604229.
Pasamontes, L.B., Torres, F.G., Zwick, D., Schafhirt, S., Muskulus, M., 2014. Support structure optimization for offshore wind turbines with a genetic algorithm-OMAE. In: Proceedings of the ASME 2014 33rd International Conference on Ocean, Offshore and Arctic Engineering. ASME. https://doi.org/10.1115/OMAE2014-24252.
Pena, B., Huang, L., 2021. Wave-GAN: a deep learning approach for the prediction of nonlinear regular wave loads and run-up on a fixed cylinder. Coast. Eng., 103902
Perez, D.H., 2012. Level Set Method Applied to Topology Optimization.
Satya Hanush, S., Manjaiah, M., 2022. Topology optimization of aerospace part to enhance the performance by additive manufacturing process. Mater. Today Proc. 62 (P14), 7373–7378. https://doi.org/10.1016/J.MATPR.2022.02.074.
Savsani, V., Dave, P., Raja, B.D., Patel, V., 2021. Topology optimization of an offshore jacket structure considering aerodynamic, hydrodynamic and structural forces. Eng. Comput. 37 (4), 2911–2930. https://doi.org/10.1007/s00366-020-00983-3.
Shi, W., et al., 2015. Soil-structure interaction on the response of jacket-type offshore wind turbine. Int. J. Precis. Eng. Manuf. Green Technol. 2 (2), 139. https://doi.org/10.1007/s40684-015-0018-7.
Stroud, W.J., 2014. Optimization of composite structures, a shape and topology sensitivity analysis. Mech. Compos. Mater. (June 2014), 307–321 [Online]. Available: http://linkinghub.elsevier.com/retrieve/pii/B9780080293844500262.
Tan, N., van Arkel, R.J., 2021. Topology optimisation for compliant hip implant design and reduced strain shielding. Materials 14 (23). https://doi.org/10.3390/MA14237184.
The Crown Estate, 2022. Offshore Wind Report.
Tian, X., Wang, Q., Liu, G., Liu, Y., Xie, Y., Deng, W., 2019. Topology optimization design for offshore platform jacket structure. Appl. Ocean Res. 84, 38–50. https://doi.org/10.1016/J.APOR.2019.01.003.
Tian, X., et al., 2022. Optimization design of the jacket support structure for offshore wind turbine using topology optimization method. Ocean Eng. 243, 110084 https://doi.org/10.1016/J.OCEANENG.2021.110084.
US Department of Energy, 2022. Offshore Wind Market Report.
US Department of Energy, 2023. A Driving FORCE for Projecting Offshore Wind Energy Costs.
Vorphal, F., Kaufer, D., 2013. Technical Report Description of a Basic Model of the UpWind Reference Jacket ' for Code Comparison in the OC4 Project under IEA Wind Annex 30. Bremerhaven, Germany.
Wang, Z., Xiang, C., Liu, H., Liu, M., 2023. Accuracy and efficiency analysis of the beam elements for nonlinear large deformation. J. Vib. Eng. Technol. 11 (1), 319–328. https://doi.org/10.1007/s42417-022-00581-1.
WindEurope, 2023. Wind Energy in Europe.
World Forum Offshore Wind, 2023. Global Offshore Wind Report.
Xie, Y.M., 2022. Generalized topology optimization for architectural design. Architect. Intell. 1 (1), 1–11. https://doi.org/10.1007/S44223-022-00003-Y, 2022 1:1.
Zhang, C., Long, K., Zhang, J., Lu, F., Bai, X., Jia, J., 2022. A topology optimization methodology for the offshore wind turbine jacket structure in the concept phase. Ocean Eng. 266 https://doi.org/10.1016/J.OCEANENG.2022.112974.
Zhu, J.H., Zhang, W.H., Xia, L., 2015. Topology optimization in aircraft and aerospace structures design. Arch. Comput. Methods Eng. 23 (4), 595–622. https://doi.org/10.1007/S11831-015-9151-2, 2015 23:4.